Spatial transcriptomics identifies novel markers of vulnerable and resistant midbrain dopamine neurons

Julio Aguila[1,#], Shangli Cheng[2,3#], Nigel Kee[1], Ming Cao[1], Qiaolin Deng[2,3]* and Eva Hedlund[1,4]*

[1] Department of Neuroscience, Karolinska Institutet, Stockholm, 171 77, Sweden

[2] Department of Physiology and Pharmacology, Karolinska Institutet, Stockholm, 171 77, Sweden

[3] Center for Molecular Medicine, Karolinska University Hospital, Stockholm, 171 77, Sweden

[4] Lead contact

[#]Equal contribution

[*]Correspondence: eva.hedlund@ki.se (E.H.) or qiaolin.deng@ki.se (Q.D.)

ABSTRACT

Defining transcriptional profiles of substantia nigra pars compacta (SNc) and ventral tegmental area (VTA) dopamine neurons is critical to understand their differential vulnerability in Parkinson Disease. However, reported transcriptional profiles for these neuron populations rely on studies in rodents and display extensive variability across small sample sizes. Here, we use laser capture microdissection coupled with RNA sequencing to analyze individually isolated SNc and VTA dopamine neurons in a large human dataset. By applying an iterative random pooling strategy as input to DESeq2, we describe a minimal cohort size that identifies 33 stably differentially expressed dopamine population-specific markers. Among these, we identify three transcripts, *ZCCHC12*, *CDH13* and *SERPINE2*, that together faithfully classify SNc or VTA dopamine neurons in both human and mouse. These novel markers will be vital for future studies aiming to distinguish the identity of stem cell-derived dopamine neurons or to induce dopamine neuron resilience.

KEYWORDS

Human midbrain dopamine neurons, spatial transcriptomics, laser microdissection, RNA sequencing, substantia nigra compacta, ventral tegmental area, Parkinson Disease

INTRODUCTION

Midbrain dopamine neurons are divided into two major populations, the substantia nigra pars compacta (SNc) and the ventral tegmental area (VTA) (Hedlund and Perlmann, 2009). SNc dopamine neurons project to the dorsolateral striatum (Dahlstroem and Fuxe, 1964) and are severely affected in Parkinson Disease (PD) (Damier et al., 1999a, b), while VTA dopamine neurons project to cortical and mesolimbic areas and are more resilient to degeneration (Hedlund and Perlmann, 2009). These neuron populations have been extensively investigated in numerous rodent models, (Bifsha et al., 2014; Chung et al., 2005; Greene et al., 2005; Grimm et al., 2004; Poulin et al., 2014), towards the goal of identifying molecular mechanisms that can prevent degeneration or to model disease. Targeted analysis of midbrain dopamine neuron populations have revealed several markers that appear to differentially label SNc e.g. *Aldh1a7*, *Sox6*, *Cbln1*, *Vav3*, *Atp2a3* and VTA e.g. *Calb1*, *Otx2*, *Crym*, *Cadm1*, *Marcks* (Bifsha et al., 2014; Chung et al., 2005; Damier et al., 1999a; Di Salvio et al., 2010; Greene et al., 2005; Grimm et al., 2004; Nichterwitz et al., 2016; Panman et al., 2014). Transcriptional analysis of human tissue has mainly been limited to SNc (Cantuti-Castelvetri et al., 2007; Simunovic et al., 2009) except for a recent small sample cohort of both SNc and VTA (Nichterwitz et al., 2016).

Results from the aforementioned studies appear to display extensive variability and seem to result in very few reproducible markers both within the same species and across mouse, rat and man, but warrants a comprehensive cross-comparative analysis. Small sample size could contribute to discrepancies, together with species-specific gene regulation, strain background, methodological differences and variability in gene expression.

To conclusively identify stable human SNc and VTA specific markers, which could reveal cell intrinsic properties underlying their differential vulnerability in PD, a thorough large-scale transcriptional profiling in adult human tissues is required. Such an analysis could also define the smallest sample size necessary to identify markers unique to each population, essential for valid study designs. Finally, identified differences could also serve as a foundation for the selective *in vitro* derivation of SNc dopamine neurons, which represent the ideal cell type for transplantation in PD (Ganat et al., 2012; Haque et al., 1997; Hedlund and Perlmann, 2009; Kriks et al., 2011; Schultzberg et al., 1984; Thompson et al., 2005).

Here we used the spatial transcriptomics method LCM-seq, which combines laser capture microdissection with polyA-based RNA sequencing (Nichterwitz et al., 2018; Nichterwitz et al., 2016), to analyze individually isolated SNc and VTA dopamine neurons from 18 human *post mortem* brains using an iterative random pooling strategy coupled with DESeq2 to reveal 33 robust population-specific markers. We show that the minimal cohort size required to reliably identify these SNc- and VTA-specific markers were eight subjects, which may explain why smaller cohorts have given inconsistent results. We further applied this approach to a large-scale data set of mouse single midbrain dopamine neurons and revealed 89 SNc and VTA stable genes. Finally, we show that three of the human population-specific markers, *ZCCHC12*, *CDH13* and *SERPINE2*, can faithfully classify SNc or VTA dopamine neurons also in the mouse. Several of the markers identified have been implicated in PD or other degenerative diseases and thus provide compelling future targets to modulate neuronal vulnerability or to model disease.

RESULTS

Bioinformatic analysis of dopamine neuron populations reveals inconsistencies across published transcriptome data sets

To understand the molecular underpinnings of the differential vulnerability among dopamine neurons, we compared previously published transcriptome studies of mouse and rat VTA and SNc dopamine neurons, using the list of markers reported as significantly up- or down-regulated (Bifsha et al., 2014; Chung et al., 2005; Greene et al., 2005; Grimm et al., 2004) or differentially expressed genes (DEGs) calculated here using DESeq2 (La Manno et al., 2016). This analysis revealed that a surprisingly low fraction of DEGs were common across data sets (Figures S1A and S1B; Tables S1 and S4). Comparing across species with our previously published small data set on human SNc and VTA (Nichterwitz et al., 2016), only two genes, *SOX6* and *CALB1*, overlapped within SNc and VTA gene lists, respectively (Figure S1C). These discrepancies highlight the urgent need to reproducibly identify signatures for VTA and SNc dopamine neurons.

Random pooling coupled with DESeq2 identify stable genes unique to the human SNc or VTA

To identify robust and specific markers in human and determine if the low number of common DEGs across previous studies was due to small sample size, we isolated VTA and SNc neurons from *post mortem* tissues of 18 adult individuals (Figures S2A-S2G; Table S2). This study represents the largest human data set profiling SNc and VTA dopamine neurons to date. The quality of human fresh frozen tissue for transcriptomic analysis may vary as a consequence of post-mortem interval (PMI), sample handling and preservation. For randomly selected samples from different cases, we confirmed that the mean cDNA libraries size of VTA and SNc samples had comparable quality (Figure S2H, I). Prior to conducting differential gene expression analysis we performed an extensive quality control to investigate the possible influence of different parameters on the gene expression (Table S5). While the total number of reads varied between individual samples, such variability was similarly distributed between SNc and VTA samples (Figure S2J). Furthermore, the number of detected genes was not correlated with the total number of reads (Figure S2K), the age of the donor (Figure S2L) or the PMI (Figure S2M). Only the number of cells collected (Figure S2N) modestly impacted gene detection (P=0.515). However, neither the number of cells collected nor the detected genes were significantly different between SNc and VTA groups (Figure S2O,P) and thus should not affect DEG identification. Analysis of marker gene expression showed that LCM-seq samples expressed the dopamine neuron markers *EN1/2*, *FOXA2*, *LMX1B*, *PITX3*, *NR4A2*, *TH* and *SLC6A3* (DAT), and the general neuronal marker NEFH, while lacking glial markers *MFGE8*, *CX3CR1* or *GPR17*, clearly demonstrating the enrichment of dopamine neurons (Figure 1A). *KCNJ6* (GIRK2) and *CALB1*, two genes often used to distinguish between SNc or VTA dopamine neurons, were present in the samples (Figure 1A), but did not separate the two dopamine neuron populations (Figure S2Q).

Differential expression analysis, considering these 18 individuals, identified 74 DEGs (Table S6), which resolved SNc from VTA neurons (Figure 1B). These genes also distinguished SNc from VTA samples from the small cohort (N=3) investigated previously (Nichterwitz et al., 2016) (Figure 1C). However, few overlapping DEGs were identified across the two studies, even though the same experimental method was used. In fact, only seven and 21 DEGs for SNc and VTA gene lists, respectively overlapped (Figure 1D). Notably, the 100 DEGs identified in the small cohort (Nichterwitz et al., 2016) (Figure S2R), failed to distinguish SNc and VTA for the

current larger cohort of 18 subjects (Figures S2S; Table S7). This suggests that sample size affects identification of DEGs and that a larger cohort size identifies DEGs that more robustly can distinguish the two populations.

To further evaluate how sample size would affect the outcome of transcriptome analysis, we developed a random pooling algorithm, and used this in combination with DESeq2, to identify the most reliable DEGs between any two populations. This approach (Figure 2A), iteratively samples an increasing proportion of a cohort of subjects, followed by differential expression analysis (DESeq2) at each iteration. Upon completion, genes are ranked according to the cumulative frequency of all iterative differential expression results. The novelty of the random pooling strategy is that it randomly choses which samples to compare for differential expression analysis and identifies the minimal number of samples required to detect robust differences between two groups. Thus this approach builds a relationship between sample size and detected DEGs. Additionally, to minimize false positives, we performed 1,000-multiple rounds of random sample selection for DESeq2 from 24 paired samples.

To reduce the biological variability, we selected only samples originating from the 12 subjects from which both SNc and VTA neurons were available. Application of the random pooling strategy to these 24 samples yielded frequency ranks of DEGs for SNc and VTA (Figures S3A and S3B; Table S8) containing multiple known human and rodent SNc and VTA markers (Bifsha et al., 2014; Cantuti-Castelvetri et al., 2007; Chung et al., 2005; Greene et al., 2005; Grimm et al., 2004; La Manno et al., 2016; Nichterwitz et al., 2016; Poulin et al., 2014; Simunovic et al., 2009). To identify the most reliable markers, we designated genes above 30% of frequency scores, as “stable genes”. The 30% cutoff was chosen as it was the minimal frequency at which at least one SNc (and one VTA) stable gene could be captured when a minimum of three individuals were used as the sampling size.

This approach identified eight stable genes for the SNc (Figure 2B) and 25 stable genes for the VTA (Figure 2C). Five SNc (labeled in red*****: *GSG1L*, *ATP2A3*, *CBLN1*, *RGS16* and *SLIT1*) and 15 VTA (in blue*****: *CADM1*, *NECAB1*, *EN2*, *TIMP2*, *GNG4*, *FXYD6*, *ZCCHC12*, *KCNIP4*, *CDH13*, *OSBPL3*, *ARHGAP26*, *PEG3*, *LYH6*, *CRYM*, *SERPINE2* and *PCSK2*) stable genes were among the aforementioned 7 and 21 overlapping DEGs, identified across two studies (Figure

1D). We also verified the validity of the genes considered stable (33 markers identified through random pooling followed by DESeq2) through a direct comparison with the outcome of DESeq2 alone applied to the same 12 subjects (Figure S3C,D). Reassuringly, all 8 SNc and 25 VTA markers perfectly overlapped with the DEGs from DESeq2 alone using an adjusted *P*-value <0.05 (Figure S3C) or a more stringent significance (adj. *P*-value <0.01, Figure S3D).

Notably, these genes were stably differentially expressed only when at least eight subjects were included in the random pooling strategy (Figure 2B, C), suggesting this to be the minimal cohort size required.

The expression of the SNc stable genes was confirmed in two independent human microarray datasets (which lacked VTA samples) (Figure S3C) (Cantuti-Castelvetri et al., 2007; Simunovic et al., 2009). Importantly, the 33 stable genes faithfully classified SNc and VTA from 21 individuals (Figure 2D), including all 18 male individuals from our current dataset and the samples from three females investigated previously (Nichterwitz et al., 2016). Using RNAscope (Figure S3D) (Wang et al., 2012) we validated the expression pattern of the SNc stable gene *SEZ6* (Figure 2E) and the VTA stable gene *CDH13* (Figure 2F), further ratifying our LCM-seq data and the random pooling approach. In conclusion, we identified novel markers that remain robust to subject variability, defining the SNc and VTA in humans and pinpoint the minimal cohort size required to detect reliable genes that distinguish these two populations.

A few stable genes define SNc and VTA dopamine neurons across species

To extend the utility of our approach and identify common stable DEGs for VTA and SNc across species, we applied the random pooling strategy to a postnatal mouse single-cell dataset profiling midbrain dopamine neurons (Figure S4A, raw data analyzed here) (La Manno et al., 2016). Single cells were initially assessed for expression of known dopamine neuron markers, the absence of contaminating glia or oligodendrocytes markers (Figure S4B) (Zhang et al., 2014) and followed by analysis using random pooling together with DESeq2 (Figure S4C). We identified 36 SNc-enriched and 53 VTA-enriched stable transcripts (Figure 3A, B; Table S9). This stable gene sets for SNc and VTA (Figures S4D and S4E, red labels) included novel genes in addition to previously reported markers (Bifsha et al., 2014; Chung et al., 2005; Greene et al., 2005; Grimm et al., 2004; La Manno et al., 2016; Nichterwitz et al., 2016; Poulin et al., 2014).

Multiple known SNc and VTA markers ranked just below our 30% frequency cutoff and were thus not designated as stable genes (Figures S4D and S4E, black labels). Importantly, the 89 stable genes identified effectively classified the single cells into the correct population (Figure S4F).

We next cross compared our human and mouse stable genes. Two genes, *ZCCHC12* and *CDH13*, were common to human and mouse VTA. In addition, *SERPINE2* was expressed in human VTA, while it's mouse homolog *Serpine2*, was expressed in the mouse SNc (Figure 3C). The expression patterns of these three genes were corroborated in the adult mouse using Allen *in situ* images (Figure 3D).

To further investigate the predictive power of these three common genes, we assessed the accuracy of our sample clustering (100% reflects perfect accuracy, while 50% reflects a random outcome). We assessed both human and mouse samples using the stable genes for each species with or without the three common genes (Figure 4A-H). As expected, when using a complete stable gene list to resolve samples within the same species, negligible reduction in the accuracy was observed after removal of the three common genes in either mouse (Figure 4A, B) or human (Figure 4E, F). Despite the low overlap of stable genes across mouse and human, they could to some extent separate samples from the other species (Figure 4C, G). However, subsequent exclusion of the three common genes led to a reduction in classification accuracy (Figure 4D, H). This was most pronounced when attempting to classify human samples using the mouse stable genes excluding *Zcchc12*, *Cdh13* and *Serpine2*, resulting in an almost chance accuracy of 56.76% (Figure 4H). Reassuringly, these three markers alone were able to largely segregate SNc from VTA samples in either species (Figure 4I, J).

In conclusion, using the random pooling approach coupled with DESeq2 we identified novel and reliable markers for the mouse SNc and VTA and revealed three common stable genes with humans that are sufficient to distinguish these two populations, on a background of dopamine neurons markers, such as DAT.

Identification and validation of genes with cross-species predictive power to resolve SNc and VTA dopamine neurons

We next sought to systematically interrogate the remaining stable SNc and VTA genes for

human and mouse that, despite not overlapping, could prove useful in cross-species classification. For a given species, we randomly excluded any three stable genes and calculated the mean accuracy of the remaining markers in resolving the other species' SNc and VTA samples (Figure 4K, L). Our random exclusion paradigm demonstrated that *SERPINE2* is the most important gene resolving mouse SNc and VTA samples, as it occupied the top rank, while *ZCCHC12* and *CDH13* occupied ranks 7 and 24, respectively (Figure 4K). Interestingly, the human stable genes *FXYD6*, *GSG1L*, *ATP2A3*, *NECAB1* and *LY6H*, were also highly ranked in their accuracy to classify mouse samples (Figure 4K). The expression patterns of these genes were corroborated in the adult mouse using Allen *in situ* images (Figures 3D and S5A).

Cdh13, *Zcchc12* and *Serpine2* were top ranked (1, 4 and 6 respectively) upon exclusion from the mouse stable gene list when resolving human samples (Figure 4L). However, only *Cdh13* strongly contributed to samples segregation followed by *Calb1*, a known VTA marker in both mouse (Chung et al., 2005; Greene et al., 2005; La Manno et al., 2016) and human (Nichterwitz et al., 2016; Reyes et al., 2012). Accordingly, the rank of *CALB1* on the human VTA list was close to the 30% frequency threshold for the "stable gene" classification (Figure S3B; Table S8).

The exclusion of other mouse stable genes, including *Slc1a2*, *Maoa*, *Tppp3*, *Lix1* and *Adrbk2*, which also fell outside of the 30% frequency threshold for human stable genes (Table S8), barely impaired the classification of human samples (Figure 4L). Similar to *Calb1*, *in situ* analysis of these genes in the adult mouse was consistent with their differential expression between VTA and SNc (Figure S5B, green labels). Many novel mouse stable genes, while displaying the expected expression patterns in line with their SNc or VTA enrichment (Figure S5B, black labels), had no impact on the classification of human samples (Figure 4L).

In conclusion, we identified additional human stable genes, including *FXYD6*, *GSG1L*, *ATP2A3*, *NECAB1* and *LY6H* with power to also distinguish SNc or VTA dopamine neurons in mouse.

DISCUSSION

To reveal the molecular signature of SNc and VTA dopamine neurons in humans, we conducted LCM-seq of single isolated neurons from *post mortem* tissues of a large human cohort. We identify 25 robust markers that define VTA and eight that distinguish SNc. Using a random pooling strategy coupled with DESeq2, we find that a minimum of eight subjects are required to identify stable genes resolving these two neuronal populations. We also applied our approach to

a single cell data set from mouse and found three overlapping stable genes with human, *ZCCHC12*, *CDH13* and *SERPINE2*, which are sufficient to classify VTA and SNc dopamine neurons in both species. Moreover, we pinpoint additional human stable genes, *FXYD6*, *GSG1L*, *ATP2A3*, *NECAB1* and *LY6H*, that can distinguish both populations in the mouse and provide a rational for future functional studies in that species.

The selective vulnerability of SNc dopamine neurons to PD and the relative resilience of VTA dopamine neurons has encouraged a number of laboratories to investigate the molecular underpinnings of these two populations with the goal of understanding neuronal vulnerability and resilience. When we analyzed existing SNc and VTA transcriptome data sets (Bifsha et al., 2014; Chung et al., 2005; Greene et al., 2005; Grimm et al., 2004; La Manno et al., 2016; Nichterwitz et al., 2016; Poulin et al., 2014), we identified large discrepancies in the reported DEGs across studies. Inconsistency among studies could depend on many factors, including sample size, which is often small. This encouraged us to conduct a large focused study on adult human midbrain dopamine neurons using LCM-seq (Nichterwitz et al., 2018). We consequently constructed the largest spatial transcriptomic human dataset of these neuron populations originating from 18 individuals. To identify stable DEGs between human SNc and VTA dopamine neurons and minimal cohort size, we developed an iterative random pooling strategy together with DESeq2, freely available (https://github.com/shanglicheng/RandomPooling) to accurately define any two cell populations.

Using a strict criteria (here 30% threshold for stable classification) to consistently retain most significant DEGs, we identified 33 robust population-specific markers only when at least eight subjects were included in the random pooling strategy. This number seems to be the minimal cohort size required and we speculate that any other two closely related populations will require similar cohort sizes to resolve subtle differences. Our findings highlight that the size among cohorts will affect the identification of lineage-specific markers, resulting in few commonly shared genes across groups and studies. This is not surprising as the one major confounding factor in human studies is the variability between subjects (Mele et al., 2015).

Further application of this methodology to a mouse single-cell dataset profiling midbrain dopamine neurons (La Manno et al., 2016), revealed 89 stable DEGs among which *Zcchc12*,

Cdh13 and *Serpine2* were in common with the human stable gene list. Interestingly, those three genes alone can distinguish between SNc and VTA neurons, on a background of general dopamine neuron markers e.g. DAT and NR4A2, in either species. These three genes are so far unexplored in the dopamine system. Serpine2 (Glia-derived nexin) is a serine protease inhibitor which can promote neurite extension by inhibiting thrombin and which appears downregulated in Alzheimer's disease (Choi et al., 1995). Serpine2 promotes biogenesis of secretory granule which is required for neuropeptide sorting, processing and secretion (Kim and Loh, 2006). *Cdh13* encodes for adhesion protein 13, which together with other family members as *Cdh9* and *Cdh15* is linked to neuropsychiatric disorders (Redies et al., 2012). Cdh13 can regulate neuronal migration and also has an effect on axonal outgrowth as demonstrated in the serotonergic system (Forero et al., 2017). Zcchc12 on the other hand is a transcriptional co-activator that positively regulates BMP signaling through interaction with Smads and CBP and appears necessary for basal forebrain cholinergic neuron gene expression (Cho et al., 2008b). When mutated, Zcchc12 appears to cause X-linked mental retardation (Cho et al., 2008a). It remains to be investigated how dopamine neurons respond to the loss of any of these three factors.

Remarkably, in spite of the low overlap between stable genes from mouse and human, we demonstrate that they have general similar features as species-specific stable genes could partly resolve SNc and VTA dopamine neurons of the other species. In fact, closely related family members are stably expressed in either species e.g. *Atp2a2*, *Cadm2*, *Ly6e*, *En1*, *Maoa* and *Pde2a* are present in the mouse while *ATP2A3*, *CADM1*, *LY6H*, *EN2*, *MAOB* and *PDE8B* are found in human.

Nevertheless, our analysis also demonstrates that there are large differences in stable genes across species. Even the shared stable marker *Serpine2*, interestingly showed an inverted expression pattern compared to its human homolog *SERPINE2*. In addition to the three common markers, several human stable genes (e.g. *FXYD6*, *GSG1L*, *NECAB1*) contributed to distinguishing mouse SNc and VTA samples. Hence, there remains a solid rational to continue investigating these human-relevant genes in the mouse.

The stable DEGs we identified here may be highly relevant to induce resistance or model disease as previously attempted in rodents (Chung et al., 2005; Poulin et al., 2014). Several of the human stable genes (or related family members) e.g. *GSG1L*, *ATP2A3*, *SLC17A6*, *RGS16*, *KCNIP1*,

CDH13, *TCF12*, *OSBPL1A*, *OSBPL10*, *GNG7*, *ARHGAP18*, *ARHGAP24*, *PCSK5*, *PEG3*, *HLA-DOA*, *HLA-DRA*, *HLA-DRB1* and *PDE8B* have been found dysregulated in PD (Bossers et al., 2009; Cantuti-Castelvetri et al., 2007; Simunovic et al., 2009) and/or are represented in PD datasets from genome wide association studies (GWASdb SNP-Disease Associations dataset, http://amp.pharm.mssm.edu). Interestingly, mice lacking *Rgs6*, a related family member of the human SNc stable gene *RGS16*, develop specific degeneration and cell loss of SNc dopamine neurons at the age of 12 months (Bifsha et al., 2014). Loss of the mouse SNc stable gene *Cplx1* results in a compromised nigrostriatal pathway in Cplx1 knockout mice (Hook et al., 2018). Moreover, mutations in the human SNc stable gene *SEZ6* has been implicated in diseases such as Alzheimer (Khoonsari et al., 2016; Paracchini et al., 2018), childhood-onset schizophrenia (Ambalavanan et al., 2016), epilepsy and febrile seizures (Mulley et al., 2011; Yu et al., 2007).

Transplantation of dopamine neurons derived from human pluripotent cell sources or fetal ventral midbrain tissue have demonstrated clinical relevance in disease models and patients (Ganat et al., 2012; Hallett et al., 2014; Kefalopoulou et al., 2014; Kirkeby et al., 2017; Kriks et al., 2011). However, there is still an urgent need to optimize the therapeutically relevant cell preparation to specifically generate SNc rather than VTA neurons for PD (Barker et al., 2017; Sonntag et al., 2018). One of the quality control guidelines to evaluate the correct patterning and differentiation of pluripotent cells to midbrain dopamine neurons is gene expression analysis using quantitative real time PCR (qPCR) or global transcriptome approaches such as RNAseq (Barker et al., 2017; Ganat et al., 2012; Nolbrant et al., 2017; Studer, 2017). Hence, having the genuine signature of adult human SNc neurons as a reference is crucial towards further advancements in the regenerative PD field. Therefore, our transcriptional analysis could serve as a reference not only to provide the specific cell identity but also the maturation properties required for meaningful disease modelling when using neurons derived from patient-specific pluripotent cells (Miller et al., 2013; Vera et al., 2016).

In summary, using LCM-seq and a random pooling approach coupled with DESeq2, we have identified robust SNc and VTA dopamine neuron markers for man and mouse. We reveal that the smallest cohort required to detect such stable DEGs consists of eight individuals, informing future studies examining highly similar cellular populations. We find that only three genes are

equally and strongly predictive across the two species, highlighting the necessity to transcriptionally define human neurons even when mouse profiles are available. This human transcriptomic data set of purified dopamine neuron subpopulations can be very valuable to deepen our understanding of neuronal vulnerability and resilience, for *in vitro* modeling of selective vulnerability and as a reference for derivation of authentic SNc neurons from stem cells.

ACKNOWLEDGMENTS

We thank Professor Abdel El Manira for critical reading of and insightful comments on the manuscript. We thank all Hedlund laboratory members for fruitful discussions. Human post-mortem tissues were kindly received from the Netherlands Brain Bank (NBB). This work was funded by grants to E.H. from Parkinsonfonden (795/15; 910/16; 991/17; 1095/18); EU Joint Programme for Neurodegenerative Disease (JPND) (529-2014-7500); Swedish Medical Research Council (Vetenskapsrådet) (2016-02112); and NEURO Sweden; by grants to Q.D. from Swedish Research Council (Vetenskapsrådet) (2014-2870); Svenska Sällskapet för Medicinsk Forskning and Jeanssons Stiftelser; Åke Wiberg, Karolinska Institutets Forskningsstiftelser and Stiftelsen; by grants to J.A. from Karolinska Institutets Forskningsstiftelser, Stiftelsen för ålderssjukdomar (2014-2018) and Åhlén-stiftelsen (mA5 h18). J.A. is supported by a postdoctoral fellowship from the Swedish Society for Medical Research and N.K. by a postdoctoral fellowship from Hjärnfonden, Sweden.

AUTHOR CONTRIBUTIONS

Conceptualization, E.H., Q.D. and J.A.; Methodology and Investigation, J.A., M.C., S.C., N.K., Q.D. and E.H.; Software, Formal Analysis and Visualization, S.C., J.A., and N.K.; Writing-Original Draft, J.A., S.C., Q.D. and E.H.; Writing-review and Editing, J.A., S.C., N.K., M.C., Q.D. and E.H.; Supervision and Project Administration, E.H. and Q.D.; Funding Acquisition, E.H., Q.D. and J.A.

DECLARATION OF INTERESTS

The authors declare no competing interests.

REFERENCES

Ambalavanan, A., Girard, S.L., Ahn, K., Zhou, S., Dionne-Laporte, A., Spiegelman, D., Bourassa, C.V., Gauthier, J., Hamdan, F.F., Xiong, L., *et al.* (2016). De novo variants in sporadic cases of childhood onset schizophrenia. Eur J Hum Genet *24*, 944-948.

Barker, R.A., Parmar, M., Studer, L., and Takahashi, J. (2017). Human Trials of Stem Cell-Derived Dopamine Neurons for Parkinson's Disease: Dawn of a New Era. Cell Stem Cell *21*, 569-573.

Bifsha, P., Yang, J., Fisher, R.A., and Drouin, J. (2014). Rgs6 is required for adult maintenance of dopaminergic neurons in the ventral substantia nigra. PLoS Genet *10*, e1004863.

Bossers, K., Meerhoff, G., Balesar, R., van Dongen, J.W., Kruse, C.G., Swaab, D.F., and Verhaagen, J. (2009). Analysis of gene expression in Parkinson's disease: possible involvement of neurotrophic support and axon guidance in dopaminergic cell death. Brain Pathol *19*, 91-107.

Cantuti-Castelvetri, I., Keller-McGandy, C., Bouzou, B., Asteris, G., Clark, T.W., Frosch, M.P., and Standaert, D.G. (2007). Effects of gender on nigral gene expression and parkinson disease. Neurobiol Dis *26*, 606-614.

Cho, G., Bhat, S.S., Gao, J., Collins, J.S., Rogers, R.C., Simensen, R.J., Schwartz, C.E., Golden, J.A., and Srivastava, A.K. (2008a). Evidence that SIZN1 is a candidate X-linked mental retardation gene. Am J Med Genet A *146A*, 2644-2650.

Cho, G., Lim, Y., Zand, D., and Golden, J.A. (2008b). Sizn1 is a novel protein that functions as a transcriptional coactivator of bone morphogenic protein signaling. Mol Cell Biol *28*, 1565-1572.

Choi, B.H., Kim, R.C., Vaughan, P.J., Lau, A., Van Nostrand, W.E., Cotman, C.W., and Cunningham, D.D. (1995). Decreases in protease nexins in Alzheimer's disease brain. Neurobiol Aging *16*, 557-562.

Chung, C.Y., Seo, H., Sonntag, K.C., Brooks, A., Lin, L., and Isacson, O. (2005). Cell type-specific gene expression of midbrain dopaminergic neurons reveals molecules involved in their vulnerability and protection. Hum Mol Genet *14*, 1709-1725.

Dahlstroem, A., and Fuxe, K. (1964). Evidence for the Existence of Monoamine-Containing Neurons in the Central Nervous System. I. Demonstration of Monoamines in the Cell Bodies of Brain Stem Neurons. Acta Physiol Scand Suppl, SUPPL 232:231-255.

Damier, P., Hirsch, E.C., Agid, Y., and Graybiel, A.M. (1999a). The substantia nigra of the human brain. I. Nigrosomes and the nigral matrix, a compartmental organization based on calbindin D(28K) immunohistochemistry. Brain *122 (Pt 8)*, 1421-1436.

Damier, P., Hirsch, E.C., Agid, Y., and Graybiel, A.M. (1999b). The substantia nigra of the human brain. II. Patterns of loss of dopamine-containing neurons in Parkinson's disease. Brain *122 (Pt 8)*, 1437-1448.

Di Salvio, M., Di Giovannantonio, L.G., Omodei, D., Acampora, D., and Simeone, A. (2010). Otx2 expression is restricted to dopaminergic neurons of the ventral tegmental area in the adult brain. Int J Dev Biol *54*, 939-945.

Forero, A., Rivero, O., Waldchen, S., Ku, H.P., Kiser, D.P., Gartner, Y., Pennington, L.S., Waider, J., Gaspar, P., Jansch, C., *et al.* (2017). Cadherin-13 Deficiency Increases Dorsal Raphe 5-HT Neuron Density and Prefrontal Cortex Innervation in the Mouse Brain. Front Cell Neurosci *11*, 307.

Ganat, Y.M., Calder, E.L., Kriks, S., Nelander, J., Tu, E.Y., Jia, F., Battista, D., Harrison, N., Parmar, M., Tomishima, M.J., *et al.* (2012). Identification of embryonic stem cell-derived midbrain dopaminergic neurons for engraftment. J Clin Invest *122*, 2928-2939.

Greene, J.G., Dingledine, R., and Greenamyre, J.T. (2005). Gene expression profiling of rat midbrain dopamine neurons: implications for selective vulnerability in parkinsonism. Neurobiol Dis *18*, 19-31.

Grimm, J., Mueller, A., Hefti, F., and Rosenthal, A. (2004). Molecular basis for catecholaminergic neuron diversity. Proc Natl Acad Sci U S A *101*, 13891-13896.

Hallett, P.J., Cooper, O., Sadi, D., Robertson, H., Mendez, I., and Isacson, O. (2014). Long-term health of dopaminergic neuron transplants in Parkinson's disease patients. Cell Rep *7*, 1755-1761.

Haque, N.S., LeBlanc, C.J., and Isacson, O. (1997). Differential dissection of the rat E16 ventral mesencephalon and survival and reinnervation of the 6-OHDA-lesioned striatum by a subset of aldehyde dehydrogenase-positive TH neurons. Cell Transplant *6*, 239-248.

Hedlund, E., and Perlmann, T. (2009). Neuronal cell replacement in Parkinson's disease. J Intern Med *266*, 358-371.

Hook, P.W., McClymont, S.A., Cannon, G.H., Law, W.D., Morton, A.J., Goff, L.A., and McCallion, A.S. (2018). Single-Cell RNA-Seq of Mouse Dopaminergic Neurons Informs Candidate Gene Selection for Sporadic Parkinson Disease. Am J Hum Genet *102*, 427-446.

Kefalopoulou, Z., Politis, M., Piccini, P., Mencacci, N., Bhatia, K., Jahanshahi, M., Widner, H., Rehncrona, S., Brundin, P., Bjorklund, A., *et al.* (2014). Long-term clinical outcome of fetal cell transplantation for Parkinson disease: two case reports. JAMA Neurol *71*, 83-87.

Khoonsari, P.E., Haggmark, A., Lonnberg, M., Mikus, M., Kilander, L., Lannfelt, L., Bergquist, J., Ingelsson, M., Nilsson, P., Kultima, K., *et al.* (2016). Analysis of the Cerebrospinal Fluid Proteome in Alzheimer's Disease. PLoS One *11*, e0150672.

Kim, T., and Loh, Y.P. (2006). Protease nexin-1 promotes secretory granule biogenesis by preventing granule protein degradation. Mol Biol Cell *17*, 789-798.

Kirkeby, A., Nolbrant, S., Tiklova, K., Heuer, A., Kee, N., Cardoso, T., Ottosson, D.R., Lelos, M.J., Rifes, P., Dunnett, S.B., *et al.* (2017). Predictive Markers Guide Differentiation to Improve Graft Outcome in Clinical Translation of hESC-Based Therapy for Parkinson's Disease. Cell Stem Cell *20*, 135-148.

Kriks, S., Shim, J.W., Piao, J., Ganat, Y.M., Wakeman, D.R., Xie, Z., Carrillo-Reid, L., Auyeung, G., Antonacci, C., Buch, A., *et al.* (2011). Dopamine neurons derived from human ES cells efficiently engraft in animal models of Parkinson's disease. Nature *480*, 547-551.

La Manno, G., Gyllborg, D., Codeluppi, S., Nishimura, K., Salto, C., Zeisel, A., Borm, L.E., Stott, S.R.W., Toledo, E.M., Villaescusa, J.C., *et al.* (2016). Molecular Diversity of Midbrain Development in Mouse, Human, and Stem Cells. Cell *167*, 566-580 e519.

Love, M.I., Huber, W., and Anders, S. (2014). Moderated estimation of fold change and dispersion for RNA-seq data with DESeq2. Genome Biol *15*, 550.

Mele, M., Ferreira, P.G., Reverter, F., DeLuca, D.S., Monlong, J., Sammeth, M., Young, T.R., Goldmann, J.M., Pervouchine, D.D., Sullivan, T.J., *et al.* (2015). Human genomics. The human transcriptome across tissues and individuals. Science *348*, 660-665.

Miller, J.D., Ganat, Y.M., Kishinevsky, S., Bowman, R.L., Liu, B., Tu, E.Y., Mandal, P.K., Vera, E., Shim, J.W., Kriks, S., *et al.* (2013). Human iPSC-based modeling of late-onset disease via progerin-induced aging. Cell Stem Cell *13*, 691-705.

Mulley, J.C., Iona, X., Hodgson, B., Heron, S.E., Berkovic, S.F., Scheffer, I.E., and Dibbens, L.M. (2011). The Role of Seizure-Related SEZ6 as a Susceptibility Gene in Febrile Seizures. Neurol Res Int *2011*, 917565.

Nichterwitz, S., Benitez, J.A., Hoogstraaten, R., Deng, Q., and Hedlund, E. (2018). LCM-Seq: A Method for Spatial Transcriptomic Profiling Using Laser Capture Microdissection Coupled with PolyA-Based RNA Sequencing. Methods Mol Biol *1649*, 95-110.

Nichterwitz, S., Chen, G., Aguila Benitez, J., Yilmaz, M., Storvall, H., Cao, M., Sandberg, R., Deng, Q., and Hedlund, E. (2016). Laser capture microscopy coupled with Smart-seq2 for precise spatial transcriptomic profiling. Nat Commun *7*, 12139.

Nolbrant, S., Heuer, A., Parmar, M., and Kirkeby, A. (2017). Generation of high-purity human ventral midbrain dopaminergic progenitors for in vitro maturation and intracerebral transplantation. Nat Protoc *12*, 1962-1979.

Panman, L., Papathanou, M., Laguna, A., Oosterveen, T., Volakakis, N., Acampora, D., Kurtsdotter, I., Yoshitake, T., Kehr, J., Joodmardi, E., *et al.* (2014). Sox6 and Otx2 control the specification of substantia nigra and ventral tegmental area dopamine neurons. Cell Rep *8*, 1018-1025.

Paracchini, L., Beltrame, L., Boeri, L., Fusco, F., Caffarra, P., Marchini, S., Albani, D., and Forloni, G. (2018). Exome sequencing in an Italian family with Alzheimer's disease points to a role for seizure-related gene 6 (SEZ6) rare variant R615H. Alzheimers Res Ther *10*, 106.

Poulin, J.F., Zou, J., Drouin-Ouellet, J., Kim, K.Y., Cicchetti, F., and Awatramani, R.B. (2014). Defining midbrain dopaminergic neuron diversity by single-cell gene expression profiling. Cell Rep *9*, 930-943.

Ramskold, D., Wang, E.T., Burge, C.B., and Sandberg, R. (2009). An abundance of ubiquitously expressed genes revealed by tissue transcriptome sequence data. PLoS Comput Biol *5*, e1000598.

Redies, C., Hertel, N., and Hubner, C.A. (2012). Cadherins and neuropsychiatric disorders. Brain Res *1470*, 130-144.

Reyes, S., Fu, Y., Double, K., Thompson, L., Kirik, D., Paxinos, G., and Halliday, G.M. (2012). GIRK2 expression in dopamine neurons of the substantia nigra and ventral tegmental area. J Comp Neurol *520*, 2591-2607.

Schultzberg, M., Dunnett, S.B., Bjorklund, A., Stenevi, U., Hokfelt, T., Dockray, G.J., and Goldstein, M. (1984). Dopamine and cholecystokinin immunoreactive neurons in mesencephalic grafts reinnervating the neostriatum: evidence for selective growth regulation. Neuroscience *12*, 17-32.

Simunovic, F., Yi, M., Wang, Y., Macey, L., Brown, L.T., Krichevsky, A.M., Andersen, S.L., Stephens, R.M., Benes, F.M., and Sonntag, K.C. (2009). Gene expression profiling of substantia nigra dopamine neurons: further insights into Parkinson's disease pathology. Brain *132*, 1795-1809.

Sonntag, K.C., Song, B., Lee, N., Jung, J.H., Cha, Y., Leblanc, P., Neff, C., Kong, S.W., Carter, B.S., Schweitzer, J., *et al.* (2018). Pluripotent stem cell-based therapy for Parkinson's disease: Current status and future prospects. Prog Neurobiol *168*, 1-20.

Studer, L. (2017). Strategies for bringing stem cell-derived dopamine neurons to the clinic-The NYSTEM trial. Prog Brain Res *230*, 191-212.

Thompson, L., Barraud, P., Andersson, E., Kirik, D., and Bjorklund, A. (2005). Identification of dopaminergic neurons of nigral and ventral tegmental area subtypes in grafts of fetal ventral mesencephalon based on cell morphology, protein expression, and efferent projections. J Neurosci *25*, 6467-6477.

Vera, E., Bosco, N., and Studer, L. (2016). Generating Late-Onset Human iPSC-Based Disease Models by Inducing Neuronal Age-Related Phenotypes through Telomerase Manipulation. Cell Rep *17*, 1184-1192.

Wang, F., Flanagan, J., Su, N., Wang, L.C., Bui, S., Nielson, A., Wu, X., Vo, H.T., Ma, X.J., and Luo, Y. (2012). RNAscope: a novel in situ RNA analysis platform for formalin-fixed, paraffin-embedded tissues. J Mol Diagn *14*, 22-29.

Yu, Z.L., Jiang, J.M., Wu, D.H., Xie, H.J., Jiang, J.J., Zhou, L., Peng, L., and Bao, G.S. (2007). Febrile seizures are associated with mutation of seizure-related (SEZ) 6, a brain-specific gene. J Neurosci Res *85*, 166-172.

Zhang, Y., Chen, K., Sloan, S.A., Bennett, M.L., Scholze, A.R., O'Keeffe, S., Phatnani, H.P., Guarnieri, P., Caneda, C., Ruderisch, N., *et al*. (2014). An RNA-sequencing transcriptome and splicing database of glia, neurons, and vascular cells of the cerebral cortex. J Neurosci *34*, 11929-11947.

Figures titles and legends

Figure 1. Gene signature of human adult midbrain dopamine neurons using LCM-seq

(A) The quality of the samples profiled in the current study was confirmed by the expression of known midbrain dopamine neuron markers *EN1/2*, *FOXA2*, *LMX1B*, *PITX3*, *NR4A2*, *TH* and *SLC6A3* (DAT), as well as the general neuronal marker neurofilament (*NEFH*), and the lack of astrocyte, microglia or oligodendroyte precursor contamination (Zhang et al., 2014).

(B) Hierarchical clustering of samples from the current study (18 male subjects) using 74 differentially expressed genes identified by DESeq2.

(C) The identified 74 differentially expressed genes also separate SNc and VTA samples from Nichterwitz et al., 2016 (3 female subjects).

(D) Venn-diagram showing overlap of the differentially expressed genes between SNc and VTA dopamine neurons found independently for each dataset.

See also Figure S2.

Figure 2. Random pooling analysis coupled with DESeq2 identify stable genes specific for human SNc and VTA dopamine neurons

(A) Schematic of the approach used to identify human stable genes using 12 subjects, including both SNc and VTA samples.

(B, C) Output of the procedure showing the probability to find stable genes for the SNc (B) and VTA (C) as a function of sample size. For each subtype, genes with an asterisk (*) are common with overlapping differentially expressed genes (Venn-diagram in Figure 1D).

(D) SNc and VTA stable genes segregate both dopamine neuron populations shown in a clustered heat map. All samples from our current study and our previous (Nichterwitz et al., 2016) study were included, n=21 subjects.

(E, F) RNAscope staining and quantification for the stable genes *SEZ6* (H, p=0.025) and *CDH13* (I, p=0.005) enriched in the SNc and VTA, respectively (n=5 subjects, data represented as mean ± SEM, Paired t test). Scale bars 30 μm (15 μm for insets).

See also Figure S3.

Figure 3. Comparison of stable genes defining SNc and VTA dopamine neurons in mouse and man

(A, B) Identification of SNc (A) and VTA (B) stable genes in the mouse dataset from La Manno et. al, 2016 using the random pooling approach coupled with DESeq2 applied to 146 single cells (73 available SNc cells and 73 randomly selected VTA cells).

(C) Venn-diagram representation showing the overlap between stable genes across mouse and man, highlighting the 3 common markers *ZCCHC12*, *CDH13* and *SERPINE2*.

(D) *In situ* hybridization images of coronal midbrain sections of the adult mouse (P56, Allen Brain Atlas) showing RNA expression pattern for *Th* and the common stable genes *Serpine2*, *Zcch12* and *Cdh13*.

Scale bars: (D) 1mm for *Th* and 200 μm for remaining markers.

See also Figure S4.

Figure 4. Predictive value of mouse and human stable genes to resolve SNc and VTA across species

(A-D) PCAs for the mouse dataset from La Manno study (n=73 SNc and 170 VTA cells) when using: mouse stable genes (A), mouse stable list after exclusion of the three common genes (B), human stable genes (C) or human stable list after exclusion of the three common markers (D), the accuracy to distinguish those populations is shown as %.

(E-H) Similar analysis as A-D but applied to human samples (subjects from our current study and Nichterwitz et al., 2016, n=21 subjects).

(I, J) The three common stable genes are sufficient to distinguish SNc and VTA samples in mouse (I) and human (J).

(K) Ranked mean accuracy for individual human stable genes, resolving the mouse dataset from La Manno et al., 2016, upon random exclusion together with any other two genes. The 3

common stable genes between mouse and human are labelled in blue, while additional genes with predictive value in the mouse are labelled in green.

(L) Ranked mean accuracy for individual mouse stable genes upon random exclusion together with any other two genes to resolve human samples (current study plus Nichterwitz et al. samples). Common stable genes between mouse and human are labelled in blue while additional genes with some predictive value in the human (led by *Calb1*) are labelled in green. See also Figure S5.

SUBJECT DETAILS

Ethics statement

We have ethical approval to work with human post-mortem samples (Tables S2 and S3) from the regional ethical review board of Stockholm, Sweden (EPN Dnr 2012/111-31/1; 2012/2091-32). Fresh frozen tissue was obtained through the Netherlands Brain Bank (NBB). The work with human tissues was carried out according to the Code of Ethics of the World Medical Association (Declaration of Helsinki).

METHOD DETAILS

Tissue sectioning and laser capture

Sample preparation prior LCM-seq was carried out as follows. Frozen midbrain tissues obtained from the brain banks were attached to chucks using pre-cooled OCT embedding medium (Histolab). 10 µm-thick coronal sections were acquired in a cryostat at -20 °C and placed onto precooled-PEN membrane glass slides (Zeiss). For RNAscope experiments, sections were cut at 12 µm-thickness and attached to Superfrost® Plus slides (Thermo Scientific). The slides with sections were kept at -20 °C during the sectioning and subsequently stored at -80 °C until further processed.

The laser capture procedure followed by sequencing library preparation (LCM-seq) was carried out as described (Nichterwitz et al., 2018; Nichterwitz et al., 2016).

Mapping and gene expression quantification

Samples were sequenced using an Illumina HiSeq2000 or HiSeq2500 platform (reads of 43 or 50 bp in length respectively). The uniquely mapped reads were obtained by mapping to the human

reference genome hg38/GRCh38 using STAR with default settings. The reads per kilobase of transcript per million mapped reads (RPKM) were estimated using "rpkmforgenes" (Ramskold et al., 2009).

As part of the quality control we verified that samples had >1 million reads and >7000 genes expressed with RPKM>1. As all samples processed exceeded this cutoff and had between 1.3~9.8 million reads and 7.9 ~ 12.3 kilo genes expressed with RPKM>1, all samples were included. The correlation coefficient between any two nearest samples was considered to be above 0.7. For cases having more than one replicate per group, corresponding samples were averaged before analysis so that each case had only one SNc and one VTA. Additionally, we confirmed the expression of known midbrain dopamine neuron markers and the purity of each sample (Figure 1A).

Differentially expressed analyses

Differentially expressed genes were identified using the R package "DESeq2" (version: 1.16.1) (Love et al., 2014) where the cutoff for significance was an adjusted P value of 0.05. Identified DEGs (from different analysis and summarized below) are shown in (Tables S4 and S6 to S9).

Table S4: Mouse differentially expressed genes (La Manno et al., 2016): 390 DEGs calculated from 73 SNc and 170 VTA cells.

Table S6: Human differentially expressed genes (current study): 74 DEGs calculated from 16 SNc and 14 VTA samples from 18 male individuals.

Table S7: Human differentially expressed genes (Nichterwitz et al., 2016): 100 DEGs calculated from 4 SNc and 3 VTA samples from 3 female subjects.

Table S8: Human stable genes: 33 DEGs calculated from 12 individuals (from the current study) using the random pooling approach.

Table S9: Mouse stable genes: 89 DEGs calculated from 73 SNc and VTA cells (La Manno et al., 2016) using the random pooling approach.

Random pooling approach coupled with DESeq2

To counteract the variability among human subjects and identify the most reliable DEGs between SNc and VTA neurons across datasets we developed a random pooling approach coupled with DESeq2 (Figure 2A; Figure S4C). The stable genes output of this analysis is

correlated with the sample size and give an unbiased estimation of the number of individuals required to consistently distinguish these closely related subpopulations. Importantly this computational tool can be used for the comparison of any other two groups (https://github.com/shanglicheng/RandomPooling, RRID:SCR_016607).

In details:

1) Define ¨N¨ and ¨M¨ as the number of samples in Group 1 and Group 2, respectively. Choose ¨I¨ as a reference representing a given number of samples from ¨N¨ and ¨M¨.

2) Define ¨i ¨ as the number of randomly selected samples from Group1 and Group2, where i ∈ {3, 4, 5, …, ¨I-1¨}. In the human dataset, as we have 12 paired samples, the i ∈ {3, 4, 5, 6, 7, 8, 9, 10, 11}.

3) Pool ¨i¨ samples (temporary considered a ¨new data set¨) and calculate DEGs with DESeq2.

4) Repeat steps 2) and 3) for ¨j¨ times (set to 1000 times in this study).

5) For every round of random selection and DESeq2, save the full list of DEGs, compute and rank their frequency.

6) Set a threshold (30% ratio in this study) to consider DEGs with higher frequency as stable genes.

Reliable genes appear when frequencies are above: Total times of random pooling x ratio (300 in this study). A stringent, but fair ratio can be defined by comparing the percentage of identified stable genes overlapping with the top (most significant) 10%, 20%, 30%, …, DEGs identified by DESeq2 alone.

Random pooling applied to human samples

To reliable identify DEGs between human SNc and VTA samples, while minimizing subject variability, we selected 12 individuals (66% of the dataset, 12 out of 18 individuals) where both neuronal populations were available and sequenced. Hence, the number of randomly selected samples (¨n¨ and ¨m¨ from ¨i¨ individuals) was from three to 11 and the algorithm repeated 1000 times (Figure 2A).

Random pooling applied to mouse single cells

For this adult mouse dataset (La Mano et. al, 2016) we defined the groups SNc (N=73 cells) and VTA (M=170 cells comprising VTA1, VTA2, VTA3 and VTA4). To compensate the unbalance in cell number and adjust dataset representation compared to the human analysis (66%), we first randomly collected a subset of 73 VTA cells, pairing both SNc and VTA. Similarly, the number of randomly selected samples was 20, 25, 30, …, 70 and the approach repeated again 1000 times (Figure S4C).

Data visualization

Data visualization was achieved using Principal Component Analysis (PCA) and Hierarchical Clustering (H-cluster).

PCA was calculated with the function "prcomp" in R with default parameters. Then, samples are projected onto the first two dimensions, PC1 and PC2. For H-cluster we used the R function "pheatmap" (version 1.0.12) with the clustering method of "ward.D2".

Accuracy calculation

To measure the power of stable genes in resolving SNc and VTA samples we calculated the clustering accuracy. This is a quantitative parameter to evaluate correct group prediction using hierarchical clustering on the first two dimensions (PC1 and PC2) of the PCA for dimensional reduction. Hierarchical clustering is performed using the ward.D2 method on the selected principal components. Ward criterion is used in the hierarchical clustering because it is based on the multidimensional variance like principal component analysis. The partitioning of samples is based on the first branch of the hierarchical tree. The genes used for PCA are different according to the evaluation purpose.

As we have two predicted groups (SNc and VTA), the minimum value for the accuracy is 50%. In details:

1) Generate PCA of SNc and VTA.

2) Hierarchically cluster the samples by using the first two principle components, PC1 and PC2. Here we can obtain a cluster tree.

3) Group the samples into predicted SNc and predicted VTA by the two main branches based on the cluster tree.

4) Define ¨N¨ and ¨M¨ as the total number of samples in Group 1 and Group 2, respectively.

5) Define ¨n¨ and ¨m¨ as the number of correctly predicted samples for Group1 and Group2, respectively.

6) Accuracy, expressed as percent, is calculated according to the formula:

Accuracy (%)= ((¨n¨+¨m¨)/(¨N¨+¨M¨)) * 100

We calculated the accuracy for six different conditions (stable gene sets) as follows:

a) Mouse stable genes applied to mouse (Figure 4A) or human (Figure 4G) samples.
b) Mouse stable genes excluding (*Zcchc12*, *Cdh13*, *Serpine2*) applied to mouse (Figure 4B) or human (Figure 4H) samples.
c) Human stable genes applied to mouse (Figure 4C) or human (Figure 4E) samples.
d) Human stable genes excluding (*ZCCHC12*, *CDH13*, *SERPINE2*) applied to mouse (Figure 4D) or human (Figure 4F) samples.
e) Human stable genes excluding three random markers applied to mouse samples (Figure 4K).
f) Mouse stable genes excluding three random markers applied to human samples (Figure 4L).

To identify additional (but not common) stable genes from mouse or human with predicted power to the other species, we performed the above analysis e) and f). Here we ranked the mean accuracy for a given stable gene upon random exclusion with any two others.

RNAscope staining of human tissues

RNAscope (Wang et al., 2012) was used to verify the expression of one SNc marker (*SEZ6*) and one VTA-preferential gene (*CDH13*) based on the sequencing data. In brief midbrain sections of human fresh frozen tissue (Table S3) were quickly thawed and fixed with fresh PFA (4% in PBS) for 1 hour at 4'C. The RNAscope 2.5 HD Assay - RED Kit (Cat. 322360) was used using manufacturer recommendations.

To evaluate the procedure in the midbrain tissue (Figure S3D), we first tested a negative control probe against a bacterial gene (Cat. 310043, *dapB*-C1) and a positive control probe against tyrosine hydroxylase (Cat. 441651, *TH*-C1). Once we set up the assay, midbrain sections were stained with *SEZ6* (Cat. 411351-C1) or *CDH13* probes (Cat. 470011-C1). Slides were counterstained with fresh 50% Gill No.1 Hematoxylin (Cat. GSH132-1L, Sigma-Aldrich) for 2

minutes, washed in water and dried for 15min at 60°C before mounting with Pertex (Cat. 00811, Histolab).

For every sample (n=5), we imaged 5-6 random fields within the SNc and VTA regions. On average 194.25±43.02 cells were imaged per region and staining. Pictures were made at 40X magnification using the bright-field of a Leica microscope (DM6000/CTR6500 and DFC310 FX camera). After randomization and coding of all the images, the number of dots within melanized cells (dopamine neurons) were counted using ImageJ (version 1.48) and later the average number of dots per cells determined for each region. Investigators performing the quantification were blinded to the sample, target region (SNc and VTA) and probe staining.

STATISTICAL ANALYSIS

For this study, statistical analyses were performed using ¨R¨. For the RNAscope analysis a paired t test (Prism 6, Version 6.0f) was used to compare the mean average dots per cell (for *SEZ6* or *CDH13* staining) between the SNc and VTA. Where applicable, individual statistical tests are detailed in the figure legends where significance is marked by $P < 0.05$. The number of subjects/cells used for each experiment is listed in the figure or figure legends. Results are expressed as mean ± SD or SEM as specified in the figure legend.

DATA AVAILABILITY

RNA sequencing data generated in this study have been submitted to the Gene Expression Omnibus (GEO) of the National Center for Biotechnology Information under the accession number GSE114918. Human samples re-analyzed from the Nichterwitz study (Nichterwitz et al., 2016) are under accession number GSE76514 and mouse adult single cells (La Manno et al., 2016) can be accessed at GSE76381. Previous human microarray studies used to verify SNc stable gene expression were accessed from the European repository ArrayExpress (E-MEXP-1416) (Cantuti-Castelvetri et al., 2007) or raw data requested to Dr. Kai C. Sonntag (Simunovic et al., 2009(Simunovic, 2009 #7).

A processed table with RPKMs values for the full dataset generated in this study can also be found at Mendeley Data under DOI 10.17632/b7nh33pdmg.1

Supplemental information titles and legends

Figure S1. Common differentially expressed genes across species. Related to tables S1 and S4.

(A) Venn diagram showing overlapping DEGs for the SNc and VTA identified in previous rat studies (Greene et al., 2005; Grimm et al., 2004).

(B) Common mouse DEGs are highlighted for the SNc and VTA from three different reports (Bifsha et al., 2014; Chung et al., 2005; La Manno et al., 2016). Samples from La Manno dataset were analyzed here with DESeq2 identifying 390 DEGs.

(C) Overlapping DEGs between rat, mouse and human (Nichterwitz et al., 2016). For rat and mouse, all previously reported DEGs were considered in spite of the variability within studies as shown in (A) and (B).

Figure S2. Quality control of human adult midbrain dopamine neurons samples profiled using LCM-seq. Related to Figure 1 and Tables S2, S5, S6 and S7.

(A to G) Nissl staining of a representative midbrain section for the isolation of SNc (B,C,D) or VTA (E,F,G) neurons before and after laser capture.

(H, I) Representative bioanalyzer profiles of cDNA libraries from VTA (H) and SNc (I) samples. The average length size for the cDNA, 700-900 base pairs, was comparable across VTA and SNc.

(J-P) The quality and similarity of samples from both populations was also interrogated based on sequencing stats, namely total reads (J) and detected genes (K). This later outcome was also correlated to biological and experimental variables such as the “Age” (L), “Post-mortem interval” (M) and “Cells” collected during the laser capture sessions (N). (O, P) While there was a modest correlation between the number of cells collected and detected genes (N, P=0.515), these variables were not significantly different between SNc and VTA groups. See also Table S5.

(Q) Hierarchical clustering of VTA and SNc samples using only *KCNJ6* (*GIRK2*) and *CALB1*.

(R, S) Samples from the Nichterwitz's study (Nichterwitz et al., 2016) were re-analyzed with DESeq2 (version 1.16.1) which identified 100-DEGs used to represent those samples (P, N=3 subjects) or our current dataset (Q, N=18 subjects).

Scale bars: 500 μm in (A), 200 μm in (B, E), 50 μm in (C,D,F,G).

Figure S3. Outcome of the random pooling coupled with DESeq2 applied to human samples and validation of SNc stables genes in the context of previous studies. Related to Figures 1, 2 and Tables S2 and S8.

(A, B) Frequency histograms (ranked by p-value), output of the random pooling approach, extend the analysis of identified SNc and VTA stable genes in human. Genes with the highest frequency (at the top, in red) represent SNc (A) and VTA (B) stable genes. Among those: *GSG1L* (Nichterwitz et al., 2016; Poulin et al., 2014), *SLIT1* (Nichterwitz et al., 2016), *SLC17A6* (Chung et al., 2005; Grimm et al., 2004; Nichterwitz et al., 2016) and *EN2* (Nichterwitz et al., 2016; Poulin et al., 2014) were previously reported as differentially expressed. Many other genes reported as differentially expressed were also found in the histograms, but at a lower frequency (not permissive to consider as stable).

(C, D) To confirm the authenticity of the genes considered stables (33 markers identified through random pooling coupled with DESeq2), Venn diagrams were used to assess the overlap with differentially expressed genes identified by DESeq2 alone applied to the same 12 subjects (C, adj. *P*-value <0.05; D, adj. *P*-value <0.01).

(E) SNc stable genes are expressed in control human SNc dopamine neurons isolated by laser capture microdissection from previous microarray studies. [#]In the study reported by Simunovic et al. (Simunovic et al., 2009), the genes *GSG1L* and *SEZ6* were not included in the array.

(F) RNAscope staining of human melanized midbrain sections using a negative control probe against a bacterial gene (*dapB*) or a positive control probe against tyrosine hydroxylase (*TH*). Scale bars: 1mm in (N) with 50 μm in insets.

Figure S4. Identification of stable genes in the mouse SNc and VTA dopamine neurons. Related to Figure 3 and Table S9.

(A) Mouse dataset used to identify stable genes in juvenile/adult (postnatal day 19 to 56) midbrain dopamine neurons. The graph shows the number of single cells sequenced for each dopaminergic population.

(B) Heat map to confirm the expression of known midbrain dopamine neuron markers and the absence of markers for other neural cells as astrocytes, microglia or oligodendrocytes.

(C) Schematic of the random pooling approach used to identify mouse stable genes from the single cell data.

(D and E) Frequency histograms (ranked by p-value) output of the random pooling approach. Identified mouse SNc (D) and VTA (E) stable genes are represented at the top (in red). Some of those stable markers have been previously identified as differentially expressed (Bifsha et al., 2014; Chung et al., 2005; Greene et al., 2005; Grimm et al., 2004; La Manno et al., 2016; Nichterwitz et al., 2016; Poulin et al., 2014). Other reported DEGs are found in the histograms but not considered stable due to their low frequency.

(F) Identified mouse stable genes separate SNc and VTA samples as visualized in the unsupervised clustering.

Figure S5. Validation of cross-species SNc and VTA dopamine neuron predictive genes. Related to Figures 3,4 and Tables S8, S9.

(A, B) *In situ* hybridization images of midbrain sections of the adult mouse (P56, Allen Brain Atlas). (A) Shown are human stable genes (in green) with predictive value in the mouse, in addition to the mouse VTA stable marker Calb1 also useful for human (see Figure 4L).

(B) Mouse stable genes with some predictive value for human (in green). The expression pattern of selected stable genes with restricted predictive value to the mouse was also verified (black labels).

Scale bars: 1mm for *Th* and 200 μm for remaining markers (applies to A, B).

Table S1. Summary of studies addressing the identity of midbrain dopamine neurons. Related to Figure S1.

Table S2. Clinical information of subjects used for LCM-seq. Related to Figures 1, 2 and S2.

Table S3. Clinical information of subjects used for RNAscope. Related to Figures 2 and S3.

Tables S4 to S9. List of DEGs, Sequencing Stats and Stable Genes (combined in 1 excel file with 6 sheets)

Table S4. List of differentially expressed genes from previous transcriptomic studies. Related to Figure S1.

Table S5. List of experimental variables and sequencing stats for the 43 samples associated with the current dataset (18 male subjects). Related to Figures 1, 2 and S2.

Table S6. List of differentially expressed genes from the current dataset (18 male subjects, 74 DEGs). Related to Figures 1 and S2.

Table S7. List of differentially expressed genes from the Nichterwitz's dataset (Nichterwitz et al., 2016) re-analyzed here (3 female subjects, 100 DEGs). Related to Figures 1 and S2.

Table S8. Full list of human stable genes/DEGs ranked by frequency identified with the random pooling approach coupled with DESeq2. Related to Figures 1, 2 and S3.

Table S9. Full list of mouse stable genes/DEGs ranked by frequency identified with the random pooling approach coupled with DESeq2. Related to Figures 3 and S4.

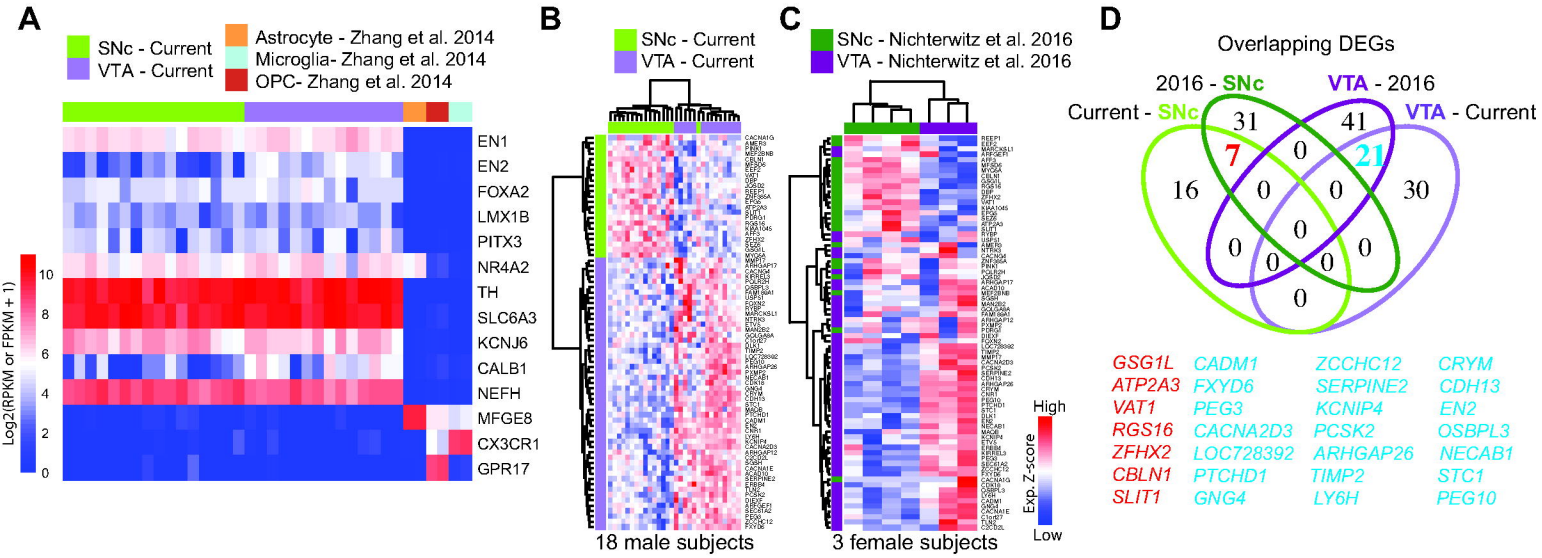
A
SNc - Current
VTA - Current
Astrocyte - Zhang et al. 2014
Microglia- Zhang et al. 2014
OPC- Zhang et al. 2014
EN1
EN2
FOXA2
LMX1B
PITX3
NR4A2
TH
SLC6A3
KCNJ6
CALB1
NEFH
MFGE8
CX3CR1
GPR17
Log2(RPKM or FPKM + 1)
B
SNc - Current
VTA - Current
18 male subjects
C
SNc - Nichterwitz et al. 2016
VTA - Nichterwitz et al. 2016
3 female subjects
High
Exp. Z-score
Low
D
Overlapping DEGs
2016 - SNc
VTA - 2016
Current - SNc
VTA - Current
31
41
7
21
16
30
GSG1L
ATP2A3
VAT1
RGS16
ZFHX2
CBLN1
SLIT1
CADM1
FXYD6
PEG3
CACNA2D3
LOC728392
PTCHD1
GNG4
ZCCHC12
SERPINE2
KCNIP4
PCSK2
ARHGAP26
TIMP2
LY6H
CRYM
CDH13
EN2
OSBPL3
NECAB1
STC1
PEG10

Figure 1

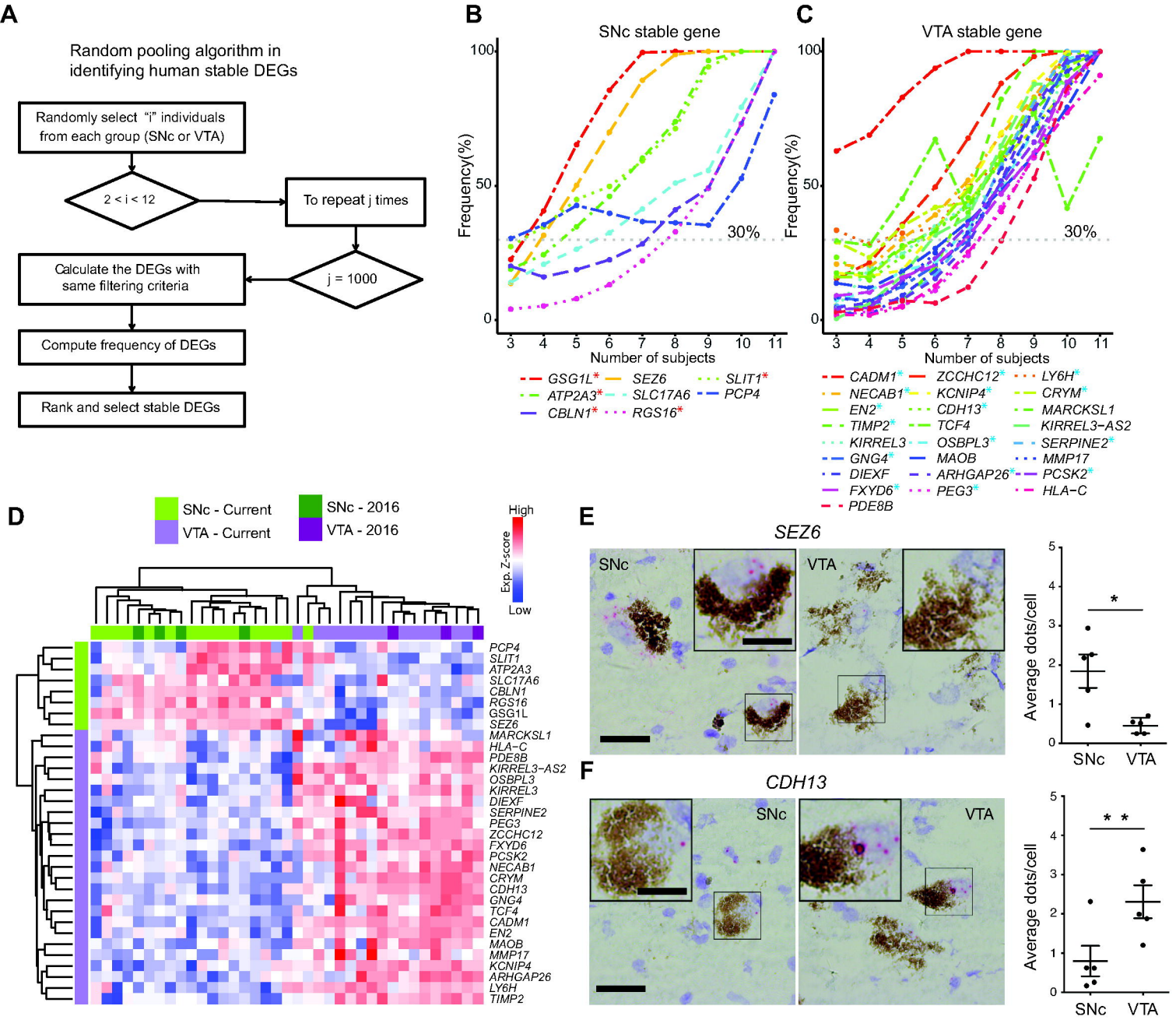
A
Random pooling algorithm in identifying human stable DEGs
Randomly select "i" individuals from each group (SNc or VTA)
2 < i < 12
To repeat j times
j = 1000
Calculate the DEGs with same filtering criteria
Compute frequency of DEGs
Rank and select stable DEGs
B
SNc stable gene
Frequency(%)
Number of subjects
30%
GSG1L* SEZ6 SLIT1* ATP2A3* SLC17A6 PCP4 CBLN1* RGS16*
C
VTA stable gene
Frequency(%)
Number of subjects
30%
CADM1* ZCCHC12* LY6H* NECAB1* KCNIP4* CRYM* EN2* CDH13* MARCKSL1 TIMP2* TCF4 KIRREL3-AS2 KIRREL3 OSBPL3* SERPINE2* GNG4* MAOB MMP17 DIEXF ARHGAP26* PCSK2* FXYD6* PEG3* HLA-C PDE8B
D
SNc - Current
VTA - Current
SNc - 2016
VTA - 2016
High
Exp. Z-score
Low
PCP4
SLIT1
ATP2A3
SLC17A6
CBLN1
RGS16
GSG1L
SEZ6
MARCKSL1
HLA-C
PDE8B
KIRREL3-AS2
OSBPL3
KIRREL3
DIEXF
SERPINE2
PEG3
ZCCHC12
FXYD6
PCSK2
NECAB1
CRYM
CDH13
GNG4
TCF4
CADM1
EN2
MAOB
MMP17
KCNIP4
ARHGAP26
LY6H
TIMP2
E
SEZ6
SNc
VTA
Average dots/cell
SNc
VTA
F
CDH13
SNc
VTA
Average dots/cell
SNc
VTA

Figure 2

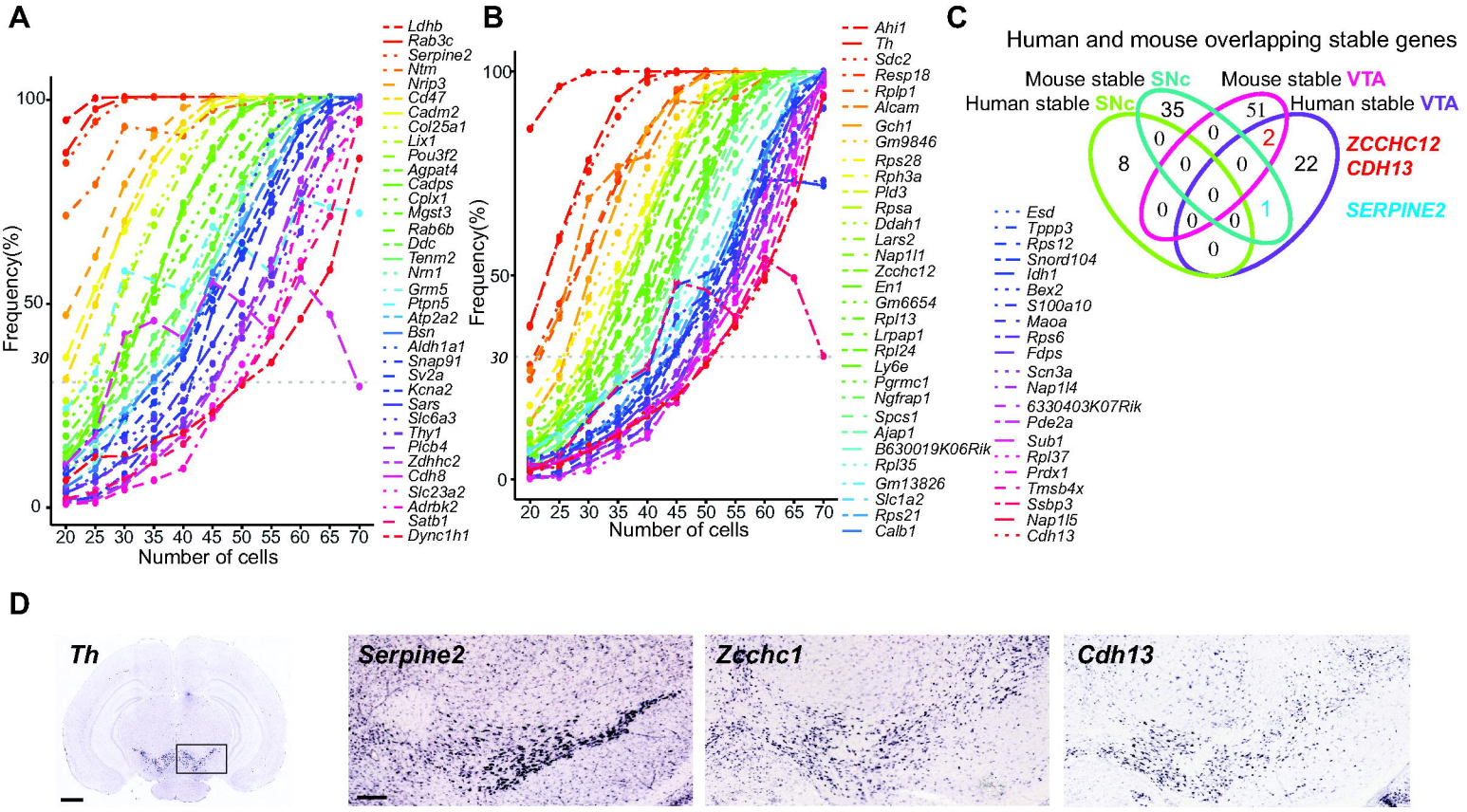
A
Frequency(%)
Number of cells
Ldhb
Rab3c
Serpine2
Ntm
Nrip3
Cd47
Cadm2
Col25a1
Lix1
Pou3f2
Agpat4
Cadps
Cplx1
Mgst3
Rab6b
Ddc
Tenm2
Nrn1
Grm5
Ptpn5
Atp2a2
Bsn
Aldh1a1
Snap91
Sv2a
Kcna2
Sars
Slc6a3
Thy1
Plcb4
Zdhhc2
Cdh8
Slc23a2
Adrbk2
Satb1
Dync1h1
B
Frequency(%)
Number of cells
Ahi1
Th
Sdc2
Resp18
Rplp1
Alcam
Gch1
Gm9846
Rps28
Rph3a
Pld3
Rpsa
Ddah1
Lars2
Nap1l1
Zcchc12
En1
Gm6654
Rpl13
Lrpap1
Rpl24
Ly6e
Pgrmc1
Ngfrap1
Spcs1
Ajap1
B630019K06Rik
Rpl35
Gm13826
Slc1a2
Rps21
Calb1
C
Human and mouse overlapping stable genes
Mouse stable SNc
Mouse stable VTA
Human stable SNc
Human stable VTA
35
51
8
22
2
1
ZCCHC12
CDH13
SERPINE2
Esd
Tppp3
Rps12
Snord104
Idh1
Bex2
S100a10
Maoa
Rps6
Fdps
Scn3a
Nap1l4
6330403K07Rik
Pde2a
Sub1
Rpl37
Prdx1
Tmsb4x
Ssbp3
Nap1l5
Cdh13
D
Th
Serpine2
Zcchc1
Cdh13

Figure 3

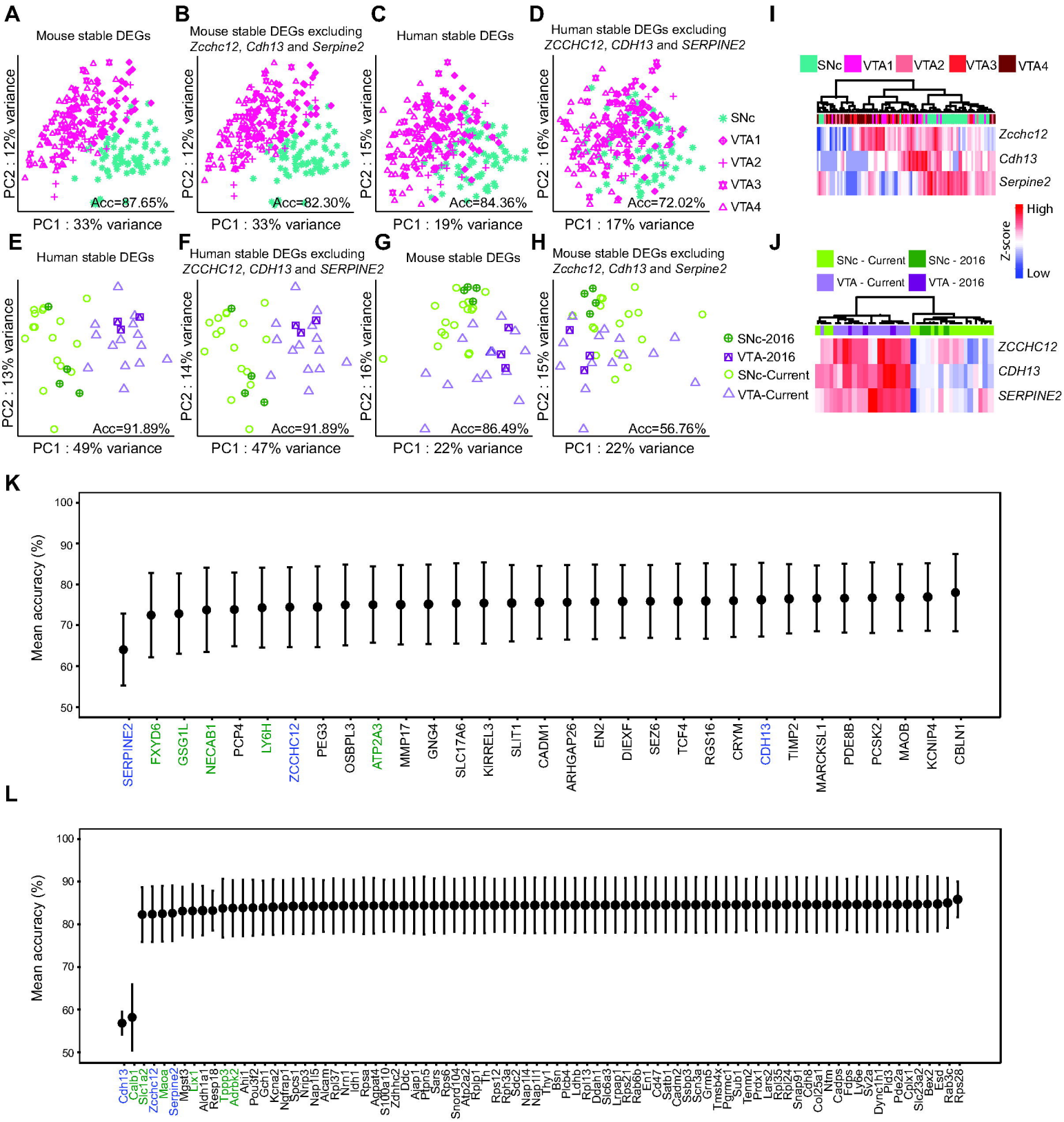
A
Mouse stable DEGs
PC2 : 12% variance
PC1 : 33% variance
Acc=87.65%
B
Mouse stable DEGs excluding
Zcchc12, Cdh13 and Serpine2
PC2 : 12% variance
PC1 : 33% variance
Acc=82.30%
C
Human stable DEGs
PC2 : 15% variance
PC1 : 19% variance
Acc=84.36%
D
Human stable DEGs excluding
ZCCHC12, CDH13 and SERPINE2
PC2 : 16% variance
PC1 : 17% variance
Acc=72.02%
SNc
VTA1
VTA2
VTA3
VTA4
I
SNc
VTA1
VTA2
VTA3
VTA4
Zcchc12
Cdh13
Serpine2
Z-score
High
Low
E
Human stable DEGs
PC2 : 13% variance
PC1 : 49% variance
Acc=91.89%
F
Human stable DEGs excluding
ZCCHC12, CDH13 and SERPINE2
PC2 : 14% variance
PC1 : 47% variance
Acc=91.89%
G
Mouse stable DEGs
PC2 : 16% variance
PC1 : 22% variance
Acc=86.49%
H
Mouse stable DEGs excluding
Zcchc12, Cdh13 and Serpine2
PC2 : 15% variance
PC1 : 22% variance
Acc=56.76%
SNc-2016
VTA-2016
SNc-Current
VTA-Current
J
SNc - Current
SNc - 2016
VTA - Current
VTA - 2016
ZCCHC12
CDH13
SERPINE2
K
Mean accuracy (%)
100
90
80
70
60
50
SERPINE2
FXYD6
GSG1L
NECAB1
PCP4
LY6H
ZCCHC12
PEG3
OSBPL3
ATP2A3
MMP17
GNG4
SLC17A6
KIRREL3
SLIT1
CADM1
ARHGAP26
EN2
DIEXF
SEZ6
TCF4
RGS16
CRYM
CDH13
TIMP2
MARCKSL1
PDE8B
PCSK2
MAOB
KCNIP4
CBLN1
L
Mean accuracy (%)
100
90
80
70
60
50
Cdh13
Calb1
Slc1a2
Zcchc12
Maoa
Serpine2
Mgst3
Lix1
Aldh1a1
Resp18
Tppp3
Adrbk2
Ahi1
Pou3f2
Gch1
Kcna2
Ngfrap1
Spcs1
Nrip3
Nap1l5
Alcam
Rpl37
Nrn1
Idh1
Rpsa
Agpat4
S100a10
Zdhhc2
Ddc
Ajap1
Ptpn5
Sars
Rps6
Snord104
Atp2a2
Rplp1
Th
Rps12
Rph3a
Sdc2
Nap1l4
Nap1l1
Thy1
Bsn
Plcb4
Ldhb
Rpl13
Ddah1
Slc6a3
Lrpap1
Rps21
Rab6b
En1
Cd47
Satb1
Cadm2
Ssbp3
Scn3a
Grm5
Tmsb4x
Pgrmc1
Sub1
Tenm2
Prdx1
Lars2
Rpl35
Rpl24
Snap91
Cdh8
Col25a1
Ntm
Cadps
Fdps
Ly6e
Sv2a
Dync1h1
Pld3
Pde2a
Cplx1
Slc23a2
Bex2
Esd
Rab3c
Rps28

Figure 4